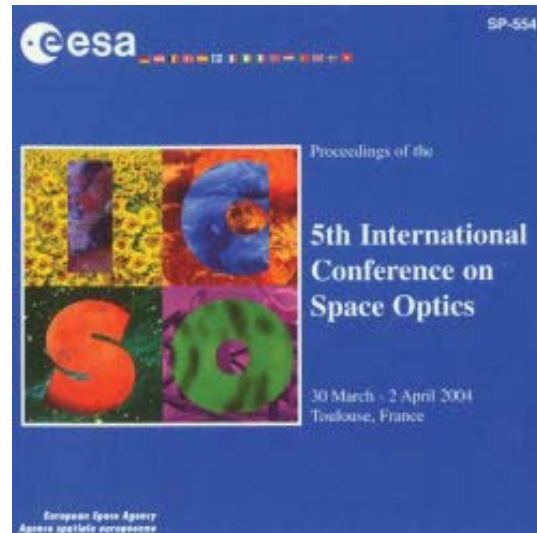


International Conference on Space Optics—ICSO 2004

Toulouse, France

30 March–2 April 2004

Edited by Josiane Costeraste and Errico Armandillo



Straylight analysis of the external baffle of COROT

J.-Y. Plesseria, E. Mazy, J.-M. Defise, P. Rochus, et al.



International Conference on Space Optics — ICSO 2004, edited by Errico Armandillo,
Josiane Costeraste, Proc. of SPIE Vol. 10568, 105680Y · © 2004 ESA and CNES
CCC code: 0277-786X/17/\$18 · doi: 10.1117/12.2307976

STRAYLIGHT ANALYSIS OF THE EXTERNAL BAFFLE OF COROT

JY. Plessier⁽¹⁾, E. Mazy⁽¹⁾, JM. Defise⁽¹⁾, P. Rochus⁽¹⁾, A. Magnan⁽²⁾, V. Costes⁽³⁾

⁽¹⁾ Centre Spatial de Liège, Av. Pré-Aily, B-4031 Liège, Belgium,
Tel. +32 4 367 6668, Fax. +32 4 367 5613, email: jyplessier@ulg.ac.be

⁽²⁾ Laboratoire d'Astrophysique de Marseille, (L.A.M.) B.P. 08, F- 13376 Marseille Cedex 12, France

⁽³⁾ Centre National d'Etudes Spatiales (CNES), 18 Avenue Edouard Belin, F-31401 Toulouse Cedex 9, France

ABSTRACT

The COROT mission is part of the program "mini-satellite" of CNES (French space agency). It implies international cooperation between European institutes and research centres. COROT aims to perform astroseismology observations and to detect exoplanets. Long duration observations of stars will be used to detect periodic variations with an afocal telescope followed by a dioptric objective and 4 CCDs. These very small variations can be caused by star seismic activities (about 10^{-6} variation of signal) or transits of planets (few 10^{-4} variation of signal).

Due to the orbit of the spacecraft (low altitude polar orbit) and even if the observations are performed in a direction perpendicular to orbit plane, the measurements can be disturbed by the straylight reflected by the earth (albedo) that can generate a periodic perturbation.

The paper details the overall optical design of the baffle. The baffle modelling and straylight computation methods are described and the expected performances are discussed.

1. INTRODUCTION

The base of COROT mission is the observation during periods up to five months of a group of stars. The variation of measured intensity will inform scientist of the seismic oscillations of stars or can indicate the transit of a planet. Separation between both effects is made by the use of a prism that can determine the spectral distribution of the variation.

The location of the spacecraft in low earth orbit is the driving parameter for the design of the baffling system. The light reflected by Earth albedo will vary during each revolution, this periodic perturbation will perturb the measurement of the periodic variation of star intensity. Even if, thanks to dedicated measurements, scientists will be able to subtract straylight signal, the mission needs to limit drastically the periodic straylight signal from Earth to very small level.

A first design of the telescope, including the baffle, has been performed by ALCATEL SPACE under CNES and LAM responsibility taking into account the envelope constraint of the launcher and optical

requirements. This study led to an afocal telescope followed by a dioptric objective and due to volume constraints the external baffle proposed is a so called 1.5-stage baffle.

When COROT has been open to international collaborations, thanks to Belgium cooperation, Centre Spatial de Liège (CSL) took the responsibility of the mechanical design and procurement of the baffle. To support that design, CSL also performed straylight analysis. Further evolutions have been implemented to improve the interface with the telescope.

2. MISSION OVERVIEW

The orbit selected for COROT is an inertial polar orbit. By observations perpendicular to the plane of the orbit, it will allow permanent view of a determined field with no occultation from Earth. During a complete observation (~150 days), the Sun will stay behind the aperture. At the end of the observation period, before the Sun goes in the forward plan, the spacecraft will rotate by 180° to observe in the other direction for a 150-day period. As a result, the Sun will again stay behind.

Around rotation of the spacecraft, some shorter observations will be performed.

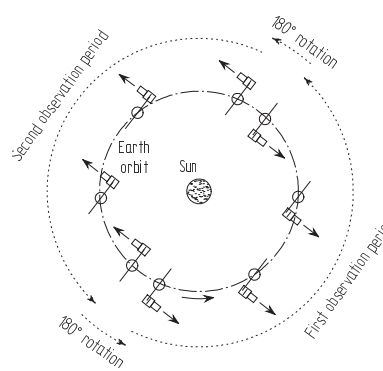


Figure 1: COROT observation principle

3. OPTICAL DESIGN DESCRIPTION

The optical design of the telescope was selected in accordance with the straylight requirements. The

selected design has an internal conjugated pupil, an intermediate image and is composed of a front baffle, an afocal telescope followed by a dioptric objective.

The 1.5 stage front baffle is dedicated for straylight attenuation of bright source above 20 degrees.

The X3 afocal telescope is composed of 2 parabolic off-axis mirror. The entrance pupil, located at the output of the front baffle, is imaged at the entrance of the dioptric objective. A mask at the intermediate focus allows a good attenuation of straylight inside the 20 degrees cone.

The dioptric objective focuses the field of view onto the focal planes. It is composed of 6 lenses.

The field of view at the focal plane assembly level is divided in 2 parts (one for seismology observation, one for planets detection) with 2 CCDs per part.

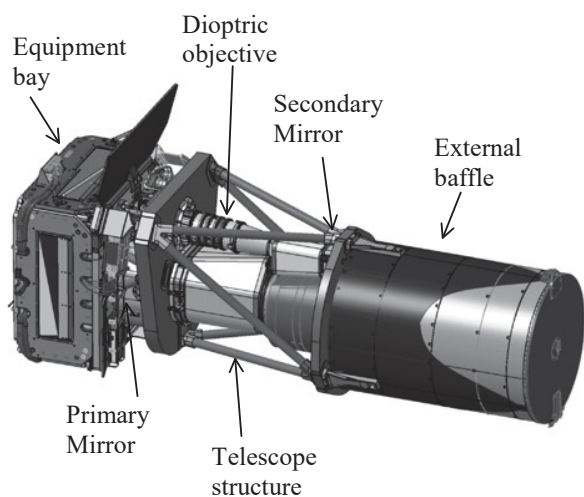


Figure 2: COROT payload (cover closed)

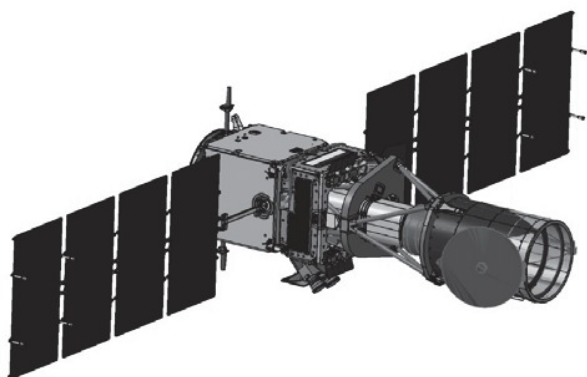


Figure 3: COROT spacecraft (cover open)

4. BAFFLE DESCRIPTION

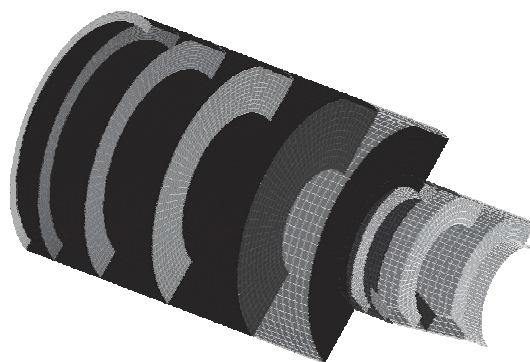
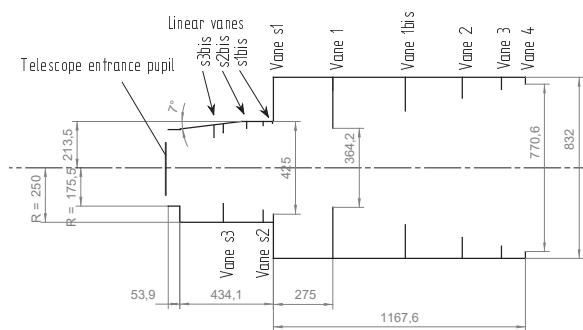


Figure 4: Optical design of the COROT baffle

The aim of the baffle is to attenuate the straylight coming from sources out of 20 degrees cone. This value has been chosen to allow off-pointing of the spacecraft in a 10° cone with respect to perpendicular to orbit in order to increase the number of potential observation targets.

A very first baffle design, optimised using ASAP and APART and in parallel with the optical design, has been proposed by CNES/LAM at the beginning of the collaboration. Some mechanical constraints have unfortunately appeared and some modifications were required, mainly in the second (smaller) tube due to the room required for the secondary mirror and its cavity. The modifications have been proposed by CNES/LAM (responsible for the straylight performances) and this new design has been analysed by CSL using ASAP.

A baffle made of two stages would have been ideal. The first stage would have prevented any light above 20 degrees from reaching the second stage. Unfortunately, the envelope problem linked to the size of the possible fairing imposes a reduction to a 1.5 stage baffle (separation being at vane 1). It means that the light up to 32.5 degrees enters the second stage and the light between 20 and 32.5 degrees is absorbed in the second stage. The total straylight is attenuated in two different

optimised elements, which is more efficient than a one-stage system.
The resulting baffle consists in two consecutive tubes containing a total of 11 vanes as shown on Figure 4.

5. INITIAL STRAYLIGHT ANALYSIS

5.1 First order analysis

The first order paths are the ones by which straylight reaches the detector after only one scattering on telescope surfaces. In the case of the COROT telescope, such surfaces do not exist. Nevertheless, first order paths have been defined as being ones with two scattering: one on a baffle wall and one on the primary mirror. The roughness and particulate contamination of the primary mirror will scatter the straylight directly in the field of view and no more attenuation will occur (with the exception of the lens transmission).

Equivalent paths can also be defined with the secondary mirror but will not be taken into account here because they occur for field angles lower than 17°.

5.2 First order analysis of the vanes

The search for critical surfaces (implied in critical paths) consists in searching surfaces which are seen by external light (i.e. that see the aperture of the baffle) and which see the primary mirror. This search has been performed with Matlab.

In the Matlab procedure written to perform this analysis, a matrix of points is drawn on the primary mirror. Then, for any observation point inside the baffle, the number of point of the mirror matrix seen without obstruction is counted. The ratio of the number of visible points to the total number of points gives the portion of primary mirror seen.

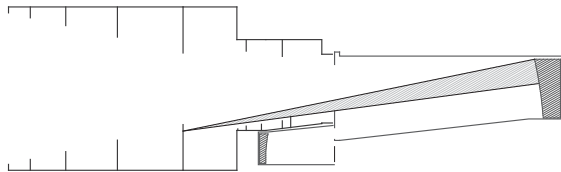


Figure 5: Portion of the primary seen by a point in the baffle

This computation can be performed for any point in the baffle. Different procedures have been written to automatically perform these computations in the planes of the vanes. By comparing the surfaces that view the mirror with the vanes, critical surfaces can be verified. Figure 6 and Figure 7 are examples of the results obtained. The grey scale indicates the percentage of primary mirror seen from black (mirror not seen) to white (full mirror seen). The two circles indicate the tube diameter and the edge of the vane. These two pictures represent the situation in the plane of chicane 1

and chicane 4 (on the face oriented towards primary mirror). It clearly shows that the edge of chicane 1 is a critical element since it can be lightened by external light and directly see almost 80 % of the primary mirror. Chicane 4 is not a problem since positive margin exists. Rapid drawing analysis shows that the edge of chicane 1 is visible for luminous object up to 32.5 degrees from optical axis.

Table 1 summarises the results of the computations. In addition to some of the edges that can be considered as critical at first order, other surfaces (back of vanes S3bis, S3, S2 and 1) are second order critical surfaces. The light can go deeper in the baffle, be scattered back to the vane rear face and than scattered again towards primary mirror. These paths add one attenuation factor (due to scattering) and will be taken into account in the global straylight analysis.

Vane #	Critical	Field of the sources
S3bis	Yes (50%)	< 20°
S3	Yes (80%)	< 21.5°
S2bis	No	-
S2	Yes (25%)	< 25.5°
S1bis	No	-
S1	No	-
1	Yes (80%)	< 32.5°
1bis	No	-
2	No	-
3	No	-
4	No	-

Table 1: First order analysis of vanes

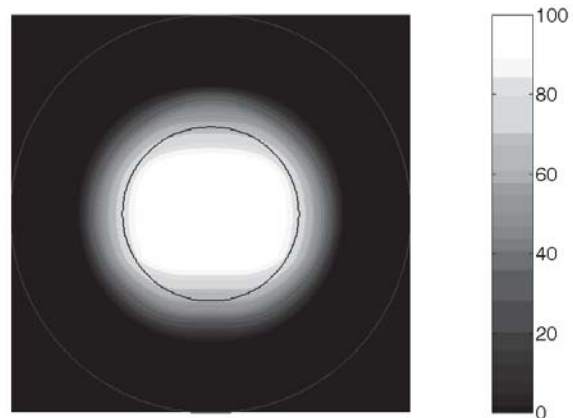


Figure 6: Chicane 1, the edge is a critical path because it sees about 80 % of primary mirror

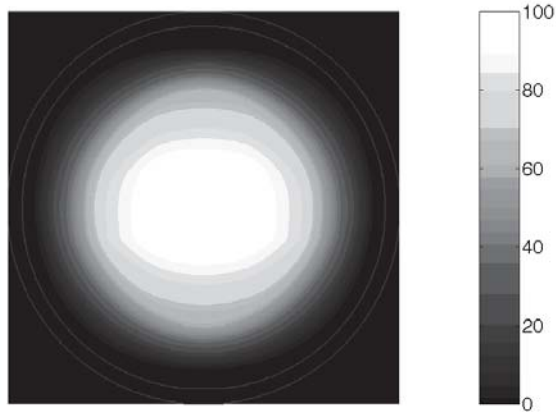


Figure 7: Chicane 4, the edge is not seen by primary mirror.

5.3 First order analysis of the tubes

The previous analysis performed for all the vanes has shown that the tubes are never seen by the primary mirror, nevertheless, we decided to further analyze the second (smaller) tube which parts can be second order critical surfaces. If they are too small, it is possible that the ray-tracing computation will not be able to detect them. The considered paths are the one with one scattering on the small tube, one on the internal tube than one on the primary mirror. For that, the Matlab procedure is modified and instead of placing a matrix on the primary mirror, it is placed once on the entrance pupil and once on the baffle aperture. We assume that all light going through the pupil will be scattered on the telescope internal tube. Moving the observation point on the small tube surface for the two cases will determine which are the surfaces seen by the aperture and by the pupil.

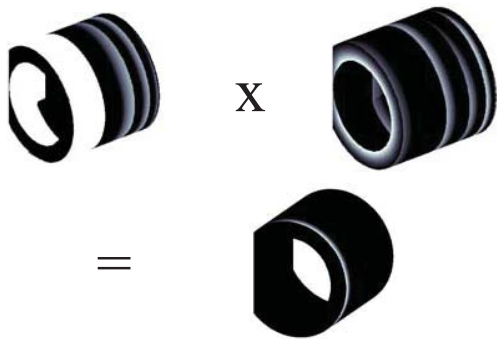


Figure 8: Detection of critical surfaces in the small tube (view from pupil times view from aperture). Only critical area is close to pupil (front of the picture)

Figure 8 shows the product of the surface viewed by the pupil by the surface viewed by the aperture of the baffle. This picture shows that the only non-null area is very close to the pupil and for very low field of view

(< 20°). This is considered not critical (unknown about the real arrangement of the connection between baffle and telescope tube could invalidate any conclusion in this area).

As a conclusion, no critical surface exists in the second tube at first order. At the second order, the area is very marginal and for low field (< 20°).

5.4 ASAP modelling

Following first (and partial second) order analysis, a ray-tracing model was run for higher level analysis with the following observation: the only critical surfaces with small area are the edges. It means that they must be analyzed separately (see 5.6).

ASAP model is geometric description, it means that no thickness has been given for the walls except for the vanes (40 μm). The junctions between all elements are supposed perfect. The modeling made by CSL should have been only done on the baffle itself but in this case, the results would have been hardly understandable in terms of performances for scientific observations. It has been decided to include in the model the afocal telescope (including entrance and exit pupil and intermediate focus) and the optical cavities of these two mirrors (they are strongly involved in the global straylight baffling performance of the payload).

The output of the computation is thus the straylight coming out of the afocal telescope and entering the dioptric objective. This can be also split in straylight in the field of view that will go directly on the detector and straylight outside the field of view that will be further scattered by the objective housing.

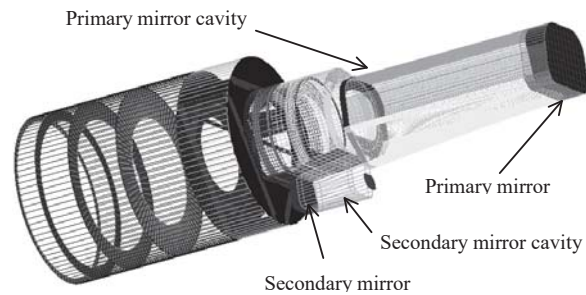


Figure 9: ASAP model for the straylight analysis.

Different coatings have been modeled by their correspondent BRDF i.e. Aeroglaze Z306 for the baffle and for the mirror cavities. The definition of the curves used is in a first approximation using data found in literature. The mirror roughness and contamination (baseline 2000 ppm) has also been modeled by their respective BRDF. Roughness modeling is based on previous measurements on representative samples and the BRDF caused by contamination has been theoretically computed using Mie scattering theory.

5.5 ASAP analysis

The main drawback of ASAP is the very high number of rays that have to be created to reach a good accuracy on the result after several scattering. CSL has made a specific effort in order to reduce the number of rays. This has been achieved by using new possibilities in ASAP and developing specific routines working with the sequential aspect of the system. The baffle has been divided in 8 sections. At the end of a section, a virtual detector has been placed to catch the rays going to the next section. Once the computation is complete in a section, the next one starts with a source being the rays caught at previous detector. This allows a high number of scatterings for the useful rays while reducing the useless rays.

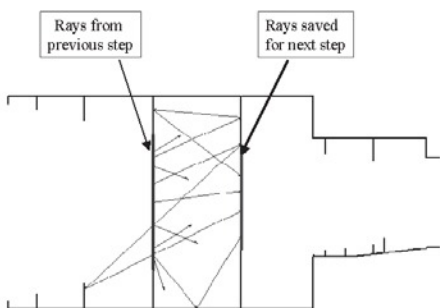


Figure 10: step-by-step analysis principle

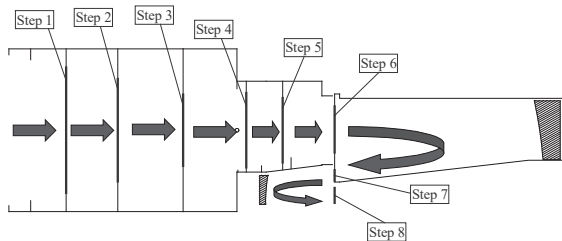


Figure 11: Model profile and separation in sections

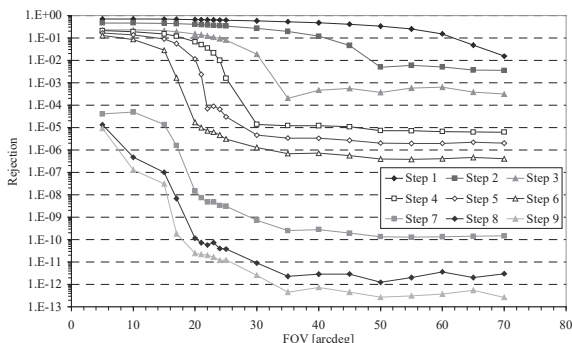


Figure 12: Results of the analysis for the different steps

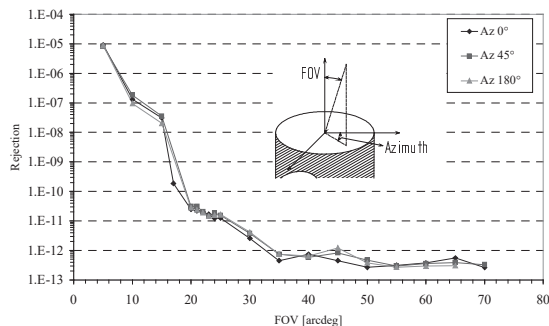


Figure 13: Results of the straylight analysis for different azimuths.

Figure 13 presents the level of straylight in the field of view of the dioptric objective. The embedded drawing representing the aperture of the baffle defines the FOV and the azimuth.

These curves indicate a good symmetry of the baffle above 20 degrees. They also reflect the geometry of the baffle: below 20°, external light directly enters into the mirror tube (FOV of the transition depends on the azimuth due to asymmetry of the pupil). Up to 27°, the light enters the smaller baffle tube, up to 32°, the light goes through the vane 1 (first stage). Above this value, the rejection is higher than 10^{12} .

These results have been used by the COROT scientific community to determine the level of straylight reaching the detector. According to these results, the selection of targets has been initiated.

5.6 Edges

As mentioned earlier, the edges can be considered as critical surfaces as it will never be possible to avoid that some part of it will see primary mirror and be lightened by external light. In a first step, the diffraction of the light by the edges has been analyzed and we rapidly concluded that diffraction was negligible in this case.

For scattering, early studies have defined the edges as flat surfaces (parallel to optical axis) with a thickness of 40 μm. These surfaces are too small to be touched statistically by rays of the global ray-tracing analysis. It was then necessary to perform a dedicated study with ASAP.

A source has been created specifically to lighten one of the edges with a sufficient number of rays and the scattered rays have been oriented preferably towards the primary mirror. Figure 14 represents resulting straylight at the level of the output pupil (FOV of dioptric objective) for all edges except vane 3 and 4. It confirms the first order analysis (Table 1), vanes 1, s2, s2bis and s3bis are the most critical ones (highest level). Nevertheless, most of that straylight will be negligible compared with the higher levels in the global scattering

analysis (Figure 13). Vane 1 is the only one generating a level of straylight comparable to the global one.

Figure 15 shows a comparison of both effect (edges straylight has been summed).

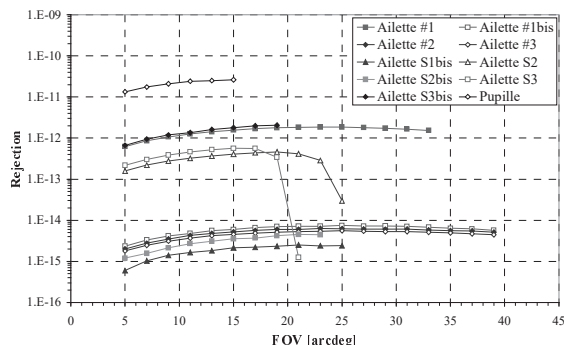


Figure 14: Level of straylight in the FOV of the dioptric objective due to edges scattering

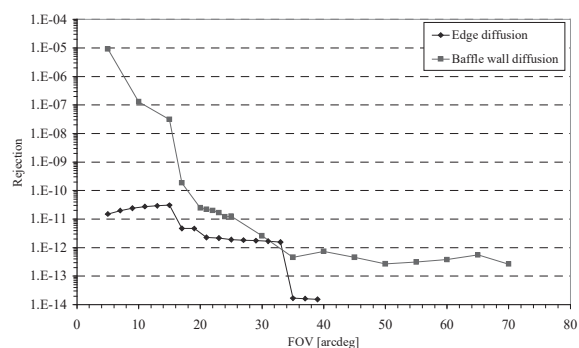


Figure 15: Comparison of levels due to global scattering and due to edges

6. SENSITIVITY TO HYPOTHESES

6.1 Introduction

Before concluding, some analyses have been performed to evaluate the sensitivity to the hypotheses and the statistical accuracy of the ray-tracing studies.

6.2 Number of rays

The first point was to determine the number of rays in the first source grid located at the entrance of the baffle. The number of rays will directly determine the duration of calculation but also the pitch of the grid and thus the size of the smallest object seen. The baseline selected size was 171 x 171 (one ray per 20 mm²). Several runs were performed for one azimuth and one field of view with different grid size. From 101 x 101 to 311 x 311 no important variation is observed.

6.3 Edges thickness

The thickness of the edges is another important point of the model. Computations have been performed with 100 μm, 40 μm and 10 μm edges.

Results clearly indicate that the straylight due to the edges is directly proportional to the thickness.

6.4 Cleanliness

Sensitivity to contamination of the mirrors will also define the margins we have on the contamination budget for the telescope and the baffle. The 2000-ppm is the value after launch as estimated by a contamination budget. Calculation with other contamination on the mirrors has been performed. Once again, a proportional behavior is observed (see Figure 16, note that the following computations are taken from a previous review of the analysis and thus the global result can differ from previous figures).

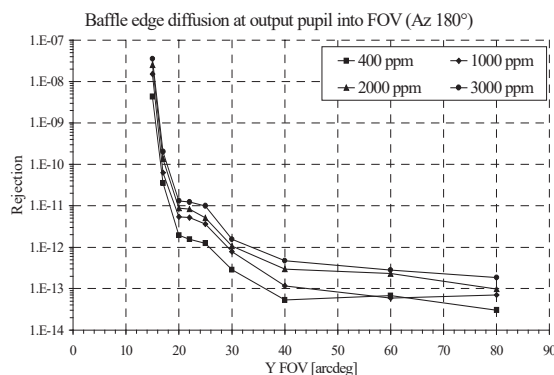


Figure 16: Variation with mirror contamination

6.5 Ray-tracing statistics

Finally, several computations were performed at the same azimuth and field of view but changing each time the statistical parameters in ASAP. The variation of the final result stays within 15 % of the average result. This variation can be considered small with respect to the factor 2 generally considered for the accuracy of the result of such analysis.

7. STRAYLIGHT DESIGN CONCLUSIONS

We can conclude that the proposed baffle has a global rejection close to the one required. The edges (mainly vane 1 edge) are considered critical and will be designed carefully. Below 20°, the rejection is driven by the primary mirror cavity and its coating. Between 20° and 27° the rejection is driven by the small tube, between 27° and 32.5°, the rejection is driven by the cavity between vanes s1 and 1 and above 32.5°, rejection is driven by the baffle up to vane 1.

The sensitivity analysis shows that the results of the computations can be considered accurate (with the classical factor 2). Major unknowns in the model are the coatings and the edges.

Further analysis at this point by the COROT science team shows that the obtained attenuation is acceptable and allows observation in a cone of ~ 20 arcdeg ($\pm 10^\circ$) around the orbit perpendicular. Nevertheless, they also observe a very high sensitivity of this limit angle value with the performances of the baffle. The straylight beyond the limit cone increases drastically. As far as possible, the real design should not be worse than the computation so that the off pointing possibilities are kept large enough.

8. MECHANICAL IMPLEMENTATION

8.1 Painting

The internal geometry of the baffle after mechanical design is in most areas in line with the optical design. Some screws and brackets are added for fixation of the vanes. The most important change is the internal stiffening structure. This structure has been correctly hidden in the cavity and is not a critical element but it will be included in an updated straylight analysis.

The important factor for the straylight analysis is also the choice of coating. The use of aluminum suggests black anodization. Some measurements indicate that the absorption of coated samples is not as good as the assumption used in ASAP. Improvement could have been reached by sandblasting the aluminum sheet. This solution has been considered too risky due to the very low thickness of the shell plate for the baffle cylinder.

The choice has thus been made to use Aeroglaze Z306 which is a well known paint for space applications. Measurements made on samples indicate that BRDF was close to the modeled one.

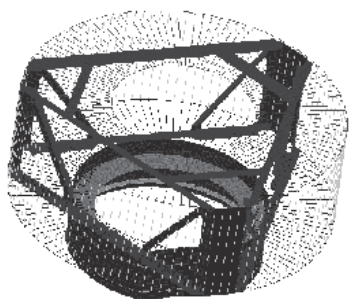


Figure 17: Internal stiffening structure between vane S1 and 1.

8.2 Edges design

Second critical point of the mechanical design is the manufacturing of the edges. Specification required a flat edge of $40 \mu\text{m}$. Different solutions have been analyzed:

stainless steel foil cut by laser or by waterjet, milled aluminum with or without paint.

The stainless steel sheet was one of the solutions, the problem was to cut the circular aperture. Both laser and waterjet techniques were tested. Laser cutting was rapidly rejected because the process creates at the edge a large local increase of thickness. The waterjet cutting resulted in a very rough edge, inducing non uniformity of the edge behavior depending on the measured location (see Figure 18). The main drawback of the stainless steel foil was also the impossibility to blacken the foil because of its very low thickness. The second solution envisaged is a milled aluminum sheet: starting from a 0.4-mm sheet, the aperture was milled using a cutting angle of 15° . The resulting edge was of very good quality. Starting from a painted edge, this process results in a large shiny surface (2 mm in the case of 0.4-sheet), moreover, the cutting of the paint could have caused adhesion problems (see Figure 20).

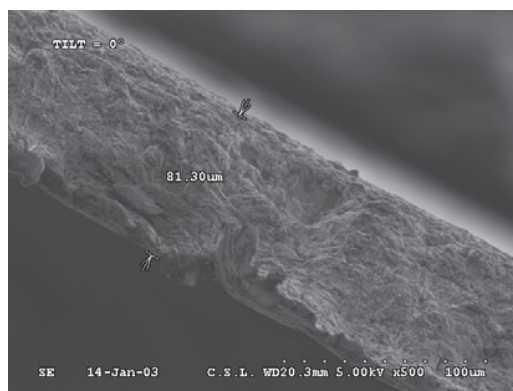


Figure 18: Waterjet cut stainless steel foil

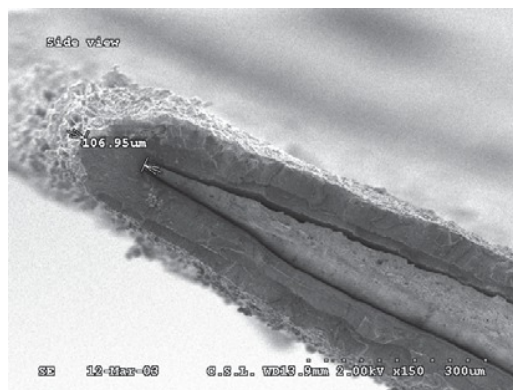


Figure 19: Milled then painted aluminium sheet

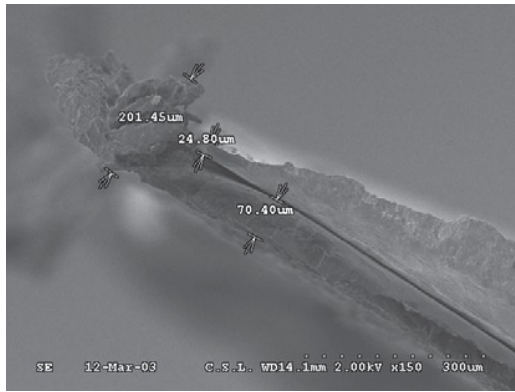


Figure 20: Painted then milled aluminium sheet

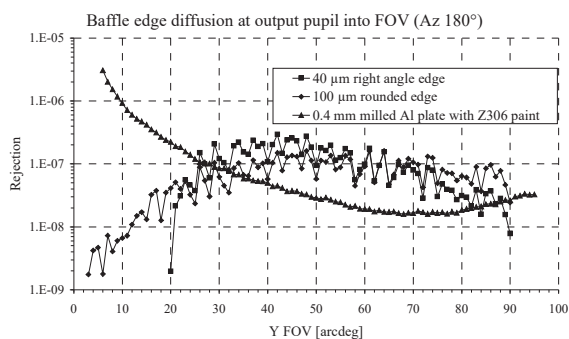


Figure 21: Comparison of measurements with computation

Another test has been performed with a sample first milled then painted (see Figure 19). The resulting thickness was higher (radius of 70 µm) and it was necessary to compare the obtained results with the original modelling of the edges. A small ASAP model has been built representing the test set-up. The 40 µm flat edge and a 100 µm rounded edges were modelled. Figure 21 shows the comparison between the different results. 40 µm flat and 100 µm rounded give similar results and the measured edge is of the same order of magnitude. This last solution has been chosen as baseline.

9. UPDATE OF STRAYLIGHT ANALYSIS

After the detailed design review of all the elements included in the optical model, an update of the straylight analysis model will be performed. It will include all the elements whose mechanical design could not fully respect the optical design. It includes coatings, edges thickness, internal stiffening structure of the baffle and some dimensions.

All elements have up to now been analysed one by one without important impact on the straylight. The global analysis will confirm this.

10. CONCLUSIONS

The different studies of the straylight analysis performed on the baffle have been detailed. This baffle goal is to attenuate straylight for fields higher than 20° in order to eliminate the periodic perturbations on measurements. This straylight is mainly coming from Earth albedo.

A first order verification has been done in order to detect critical surfaces that could not be detected by the global model. With it, it was also possible to perform a selection of the points that required and will require special attention (e.g. edges).

The analysis has been performed with an original technique that allows computation on a large structure to very high rejection factors. The results of the analysis show a good correlation with the geometry of the baffle. Then the mechanical implementation is shortly discussed with some attention on the points considered critical with respect to straylight. Finally, the updated model is introduced.

Our studies confirm the very high straylight performance of our baffle and lead us being confident on the final global straylight rejection of COROT payload and its compliance with the scientific need.

11. AKNOWLEDGMENT

The Belgian contribution to the COROT program is funded by the Federal Science Policy Office, in the frame of the ESA/Prodex program.

12. REFERENCES

List of papers about COROT can be found on http://www.astrsp-mrs.fr/projets/corot/arti_corot.html.

Additional information can be found on CNES website: <http://smc.cnes.fr/COROT/Fr/>

1. F. Paoli, F. Douillet, M. Jouret-Perl, J.B. Dubois, "COROT: a small satellite in low earth orbit for asteroseismology and the search of exoplanets", 50th International Astronautical Congress, 4-8 Oct 1999, Amsterdam, The Netherlands, IAF-99-Q.1.02.

2. A. Baglin, M. Auvergne, C. Catala, E. Michel and the Corot Team, "Asteroseismology with the Space mission COROT: photometric performances, targets and mission profile", SOHO/GONG workshop, Tenerife, October 2000

3. JY. Plessier, E. Mazy, JM. Defise, P. Rochus, E. Lemmens, D. Vrancken, "Optical and mechanical design of a straylight rejection baffle for COROT", Proceedings of SPIE, Vol. 5170, San Diego, 2003